Two Cytoplasmic Effectors of *Phytophthora sojae* Regulate Plant Cell Death via Interactions with Plant Catalases[1]

Meixiang Zhang, Qi Li, Tingli Liu, Li Liu, Danyu Shen, Ye Zhu, Peihan Liu, Jian-Min Zhou, and Daolong Dou*

Department of Plant Pathology, Nanjing Agricultural University, Nanjing 210095, China (M.Z., Q.L., T.L., L.L., D.S., Y.Z., P.L., D.D.); and Center for Genome Biology and State Key Laboratory of Plant Genomics, Institute of Genetics and Developmental Biology, Chinese Academy of Sciences, Beijing 100101, China (Q.L., J.-M.Z.)

Plant pathogenic oomycetes, such as *Phytophthora sojae*, secrete an arsenal of host cytoplasmic effectors to promote infection. We have shown previously that *P. sojae* PsCRN63 (for crinkling- and necrosis-inducing proteins) induces programmed cell death (PCD) while PsCRN115 blocks PCD in planta; however, they are jointly required for full pathogenesis. Here, we find that PsCRN63 alone or PsCRN63 and PsCRN115 together might suppress the immune responses of *Nicotiana benthamiana* and demonstrate that these two cytoplasmic effectors interact with catalases from *N. benthamiana* and soybean (*Glycine max*). Transient expression of *PsCRN63* increases hydrogen peroxide (H_2O_2) accumulation, whereas PsCRN115 suppresses this process. Transient overexpression of *NbCAT1* (for *N. benthamiana CATALASE1*) or *GmCAT1* specifically alleviates PsCRN63-induced PCD. Suppression of the PsCRN63-induced PCD by PsCRN115 is compromised when catalases are silenced in *N. benthamiana*. Interestingly, the NbCAT1 is recruited into the plant nucleus in the presence of PsCRN63 or PsCRN115; NbCAT1 and GmCAT1 are destabilized when PsCRN63 is coexpressed, and PsCRN115 inhibits the processes. Thus, PsCRN63/115 manipulates plant PCD through interfering with catalases and perturbing H_2O_2 homeostasis. Furthermore, silencing of catalase genes enhances susceptibility to *Phytophthora capsici*, indicating that catalases are essential for plant resistance. Taken together, we suggest that *P. sojae* secretes these two effectors to regulate plant PCD and H_2O_2 homeostasis through direct interaction with catalases and, therefore, overcome host immune responses.

To infect host plants, phytopathogens secrete a battery of effectors to interfere with the plant immune system, resulting in effector-triggered susceptibility (Hann et al., 2010; Dou and Zhou, 2012; Rafiqi et al., 2012). A growing number of effectors that contribute to pathogen virulence have been reported. For example, to suppress host immune responses, bacterial pathogens deliver effector proteins into the host cytoplasm through a specialized type III secretion apparatus (Hann et al., 2010). Filamentous fungi and oomycetes secrete effectors, which are either translocated into the host cytoplasm or act in the plant apoplast to interfere with a wide range of host physiological processes (Kamoun, 2006; Dou and Zhou, 2012; Rafiqi et al., 2012). The effectors secreted by these distinct pathogen groups can target diverse host immune signaling pathways, such as plant programmed cell death (PCD; Dou and Zhou, 2012).

Phytopathogenic oomycetes cause some of the most destructive plant diseases globally. For example, *Phytophthora sojae* causes soybean (*Glycine max*) root and stem rot, leading to substantial annual yield losses (Tyler, 2007). Many *Phytophthora* spp. pathogens are hemibiotrophs that mostly initiate the infection cycle as biotrophs but switch to a necrotrophic lifestyle at later stages. However, little is known about the molecular mechanisms that promote each phase, nor those that regulate the transition between the two stages. Recent advances in effector biology revealed that this process is likely determined by the sequential delivery of functionally distinct effectors into host plant cells (Koeck et al., 2011). For example, to establish a biotrophic interaction with the host, *Phytophthora infestans* produces SUPPRESSOR OF NECROSIS1 at the early infection stages and suppresses PCD triggered by other elicitors, and it later switches to a necrotrophic lifestyle (Kelley et al., 2010). *P. sojae* delivers effectors with contrasting biological activities to sequentially promote infection (Wang et al., 2011). Oomycete pathogens can secrete hundreds of cytoplasmic effectors, including RxLRs (for Arg, any amino acid, Leu, and Arg) and CRNs (for crinkling- and necrosis-inducing proteins). However, it is difficult to predict their functions due to a lack of sequence similarity to known enzymes or proteins. Two notable exceptions are the *P. sojae* avirulence protein 3b (AVR3b),

[1] This work was supported by the National Natural Science Foundation of China (grant nos. 31371894 and 31301613) and the Natural Science Foundation of Jiangsu Province (grant no. BK2012027).

* Address correspondence to ddou@njau.edu.cn.

The author responsible for distribution of materials integral to the findings presented in this article in accordance with the policy described in the Instructions for Authors (www.plantphysiol.org) is: Daolong Dou (ddou@njau.edu.cn).

www.plantphysiol.org/cgi/doi/10.1104/pp.114.252437

which contains a domain with similarity to Nudix hydrolases (Dong et al., 2011), and *P. infestans* CRN8, which exhibits kinase activity (van Damme et al., 2012).

The identification of host targets remains an essential approach to elucidate effector functions. The functional mechanisms of several *P. infestans* effectors have been discovered using this strategy. PiAVR3a manipulates plant immunity by interacting with and stabilizing the host E3 ligase CMPG1 (for a U-box E3 ligase with a conserved Cys/Met/Pro/Gly amino acid motif in its sequence; Bos et al., 2010). PiAVRblb1 may target the plant lectin receptor kinase LecRK-I.9 to interfere with the cell wall and plasma membrane continuum and promote infection (Bouwmeester et al., 2011). PiAVRblb2 prevents the secretion of the plant immune protease C14 by interacting with it at the haustorial interface (Bozkurt et al., 2011). A *P. infestans* RxLR effector, PITG_03192, interacts with NAC (an acronym for NAM [No Apical Meristem], ATAF1-2, and CUC2 [Cup-Shaped Cotyledon]) transcriptional factors in *Nicotiana benthamiana* and prevents their relocalization from the endoplasmic reticulum to the nucleus (McLellan et al., 2013). The avirulence effector PiAVR2 associates with plant phosphatase BSU-LIKE PROTEIN1, and the complex can be recognized by the resistance protein R2, resulting in effector-triggered immunity (Saunders et al., 2012). However, the targets of the *P. sojae* effectors and oomycete CRN effectors have not been reported.

CRNs, a major class of oomycete cytoplasmic effectors, were originally identified following an in planta functional expression screen for candidate secreted proteins of *P. infestans* (Torto et al., 2003). Transient expression of several CRNs causes PCD in plants (Schornack et al., 2010; Rajput et al., 2014). Analogous to RxLR effectors, the N-terminal region of CRN proteins contains a conserved FLAK motif, which is known to be required for CRN effector translocation into the host plant cells (Schornack et al., 2010). Similar to RxLR effectors, the C termini of CRNs are diverse and required for virulence (Haas et al., 2009). The majority of CRN effectors are thought to cause PCD in plants; however, recent studies demonstrated that few CRNs induce PCD in plants and that the majority of CRNs suppress PCD induced by distinct elicitors (Shen et al., 2013; Stam et al., 2013). PsCRN63 and PsCRN115 were identified in *P. sojae* and found to be essential for the full virulence of the pathogen. Although sharing 95.7% identity at the amino acid level, they possess contrasting biological activities on *N. benthamiana* and soybean. Specifically, PsCRN63 induces PCD while PsCRN115 blocks it (Liu et al., 2011). The underlying mechanisms, however, remain unknown.

Hydrogen peroxide (H_2O_2), a reactive oxygen species (ROS), is a regulator of many physiological processes, including disease resistance (Petrov and Van Breusegem, 2012). The biological function of H_2O_2 is dependent on its concentration. Generally speaking, a low level of H_2O_2 serves as a signaling molecule, whereas high levels provoke cell death (Gough and Cotter, 2011). Inhibition of host H_2O_2-mediated resistance by pathogen effectors may be an effective strategy to suppress plant immunity (Hemetsberger et al., 2012). Catalases present in the majority of living organisms convert H_2O_2 into water and oxygen. In Arabidopsis (*Arabidopsis thaliana*), the *CATALASE* gene family includes three members (*CAT1*, *CAT2*, and *CAT3*). CAT2 and CAT3 are localized to the peroxisome and function as major H_2O_2 scavengers that contribute to ROS homeostasis (Du et al., 2008). LESION SIMULATING DISEASE1 (LSD1) interacts physically and genetically with catalases to regulate PCD in Arabidopsis (Li et al., 2013). Thus, catalases may play an important role in plant H_2O_2 homeostasis, PCD, and resistance.

Here, we report that both PsCRN63 and PsCRN115 of *P. sojae* interacted directly with catalases and relocated these enzymes from the peroxisomes to the nucleus in *N. benthamiana*. PsCRN63 promotes plant PCD, which may result from its ability to down-regulate catalase stability and up-regulate H_2O_2 levels. PsCRN115, however, counteracts the functions of PsCRN63. Our results suggest that PsCRN63 and PsCRN115 interact in opposing manners to regulate H_2O_2 homeostasis and PCD.

RESULTS

Expression of PsCRN63 or PsCRN63/115 Promotes the in Planta Growth of *Phytophthora capsici*

Silencing of *PsCRN63/115* jointly reduced *P. sojae* virulence (Liu et al., 2011). To further determine the role of PsCRN63 and PsCRN115 during pathogen infection, we used an in planta transient assay. In this assay, pBinGFP2 empty (*GFP* alone) was expressed in one-half of an *N. benthamiana* leaf via agroinfiltration, and *PsCRN63* and *PsCRN115* were expressed as GFP fusions separately or coexpressed in the other half of the leaf. Leaves were inoculated with *P. capsici* zoospores 12 h after infiltration. The average lesion diameters were recorded at 24 h after inoculation (Fig. 1). All of the inoculated leaves showed typical water-soaked lesions (Fig. 1A), suggesting that PsCRN63 and PsCRN115 could not impair *P. capsici* penetration. However, the results clearly showed that, compared with the GFP expression control, the expression of *PsCRN63* in *N. benthamiana* cells significantly enhanced *P. capsici* colonization. In contrast, the expression of PsCRN115 promoted resistance to the *Phytophthora* spp. pathogen. Interestingly, coexpression of both CRN effectors enhanced the susceptibility of *N. benthamiana* to *P. capsici* infection (Fig. 1). To confirm the expression of the effector genes, the GFP fluorescence of the fusion proteins was observed using a confocal laser scanning microscope, and nuclear localization of fluorescent signals showed that GFP-effector fusion proteins were expressed (Fig. 1B). These results suggest that PsCRN63 alone or together with PsCRN115 can act within plant cells to promote effector-triggered susceptibility.

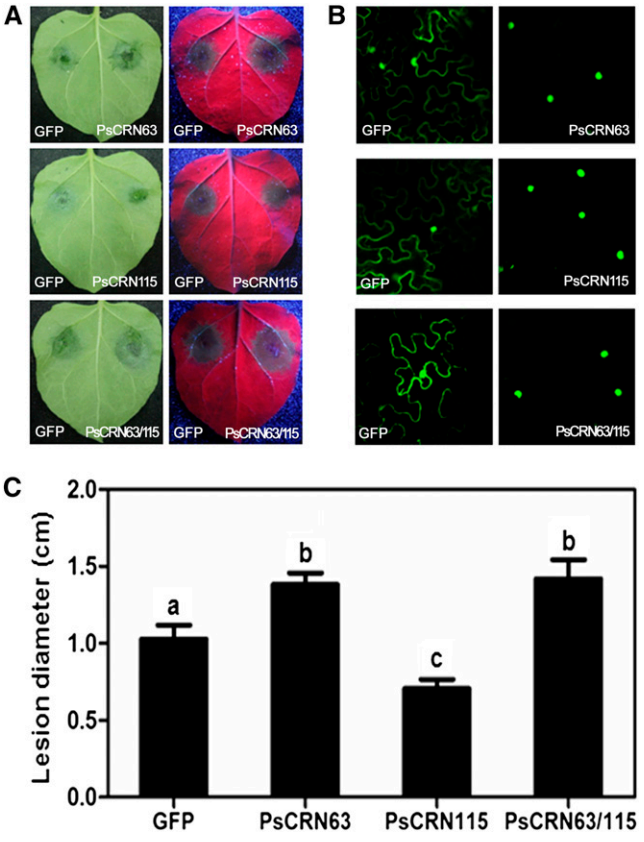

Figure 1. Expression of *PsCRN63* or *PsCRN63/PsCRN115* in planta enhanced the susceptibility of *N. benthamiana* to *P. capsici*. A, Leaf phenotypes upon *P. capsici* infection. *A. tumefaciens* was used to transiently express the indicated CRN effectors (*PsCRN63* or *PsCRN115* alone or coexpressing both effectors) as GFP fusions on one-half of an *N. benthamiana* leaf and free *GFP* on the other. Leaves were infected with *P. capsici* zoospores 12 h after infiltration. Typical photographs were taken 24 h after inoculation under normal light (left) and UV light (right). B, Nuclear localization of GFP florescence signals in the infiltrated leaves. The infiltrated leaves were detached at 24 h after infiltration, and GFP fluorescence was detected using a confocal laser scanning microscope. C, Average lesion diameters of *N. benthamiana* leaves expressing CRN effectors or *GFP*. Error bars represent SE calculated from at least 11 independent biological replicates. The letters indicate significant differences ($P < 0.01$) determined by a nonparametric Kruskal-Wallis test.

PsCRN63/115 Associates with CATs from *N. benthamiana* and Soybean

To investigate the molecular mechanisms underlying the regulation of plant PCD and resistance responses by PsCRN63 and PsCRN115, we identified potential protein targets in *N. benthamiana* using in planta coimmunoprecipitation (co-IP) followed by liquid chromatography-tandem mass spectrometry (LC-MS/MS) analysis (Supplemental Table S1). We identified two proteins, a homolog of HSP90 (NbHSP90) and a catalase (NbCAT1), that may associate with PsCRN63/115 because they were not found in the GFP control (Supplemental Table S1). We then examined the interaction between these two candidates and the CRN effectors using a yeast (*Saccharomyces cerevisiae*) two-hybrid assay. Figure 2A shows that NbCAT1, but not HSP90, interacted with both PsCRN63 and PsCRN115. Furthermore, co-IP was conducted to confirm the interaction between NbCAT1 and these two CRN effectors in Arabidopsis protoplasts. The result showed that both PsCRN63 and PsCRN115 were associated with NbCAT1 (Fig. 2B). In contrast, PsCRN127, a randomly selected CRN effector from *P. sojae*, did not coprecipitate with NbCAT1. PsCRN63 or PsCRN115 did not coprecipitate with two other Arabidopsis proteins, BOTRYTIS-INDUCED KINASE1 (BIK1) and ENHANCED DISEASE SUSCEPTIBILITY1 (EDS1), indicating that interactions between PsCRN63/115 and NbCAT1 were specific.

The search for genomic sequences homologous to NbCAT1 (NbS00013764g0007.1) revealed seven putative CATs in *N. benthamiana* genome databases and four in soybean genome databases. Protein sequence alignment showed that catalases are conserved among *N. benthamiana* and soybean (Supplemental Fig. S1). We cloned three other CATs (NbS00003826g0005.1, NbCAT2; NbS00015038g0018.1, NbCAT3; and NbS00006116g0019.1, NbCAT4) from *N. benthamiana* and two (Glyma14g39810.1, GmCAT1; and Glyma04g01920.1, GmCAT2) from soybean and then examined the interactions between the CRN effectors and these catalases using co-IP. The results showed that both CRN effectors interacted with all of the tested proteins, including four from *N. benthamiana* and two from soybean (Fig. 2C). Our results suggested that PsCRN63/115 interacted with plant catalases.

PsCRN63 and PsCRN115 Interact with Catalase in the Plant Nucleus

PsCRN63 and PsCRN115 are localized to the plant cell nucleus (Liu et al., 2011). However, catalases are usually enriched in the cytoplasm and peroxisomes (Mhamdi et al., 2010). We found that *N. benthamiana* NbCAT1 colocalized with a peroxisome marker protein (Nelson et al., 2007; Fig. 3A), confirming the peroxisome localization of NbCAT1. To determine the subcellular site(s) where the two CRN effectors interact with a plant catalase, we transiently coexpressed GFP:CRN and mCherry:NbCAT1 fusions via agroinfiltration in *N. benthamiana* leaves. Strong mCherry fluorescent signals were detected in the nucleus, overlapping with the GFP:CRN signals (Fig. 3B), indicating that NbCAT1 was relocated to the nucleus by PsCRN63 or PsCRN115. Transient expression of GFP:PsCRN63 fusion protein induced cell death in *N. benthamiana* leaves, and the cell death could be suppressed by GFP:PsCRN115, indicating that the functionality of the GFP-tagged effectors was not affected (Supplemental Fig. S2). These results suggested that, although both PsCRN63 and PsCRN115 can relocate NbCAT1 from the peroxisomes to the nucleus, the two effectors play different

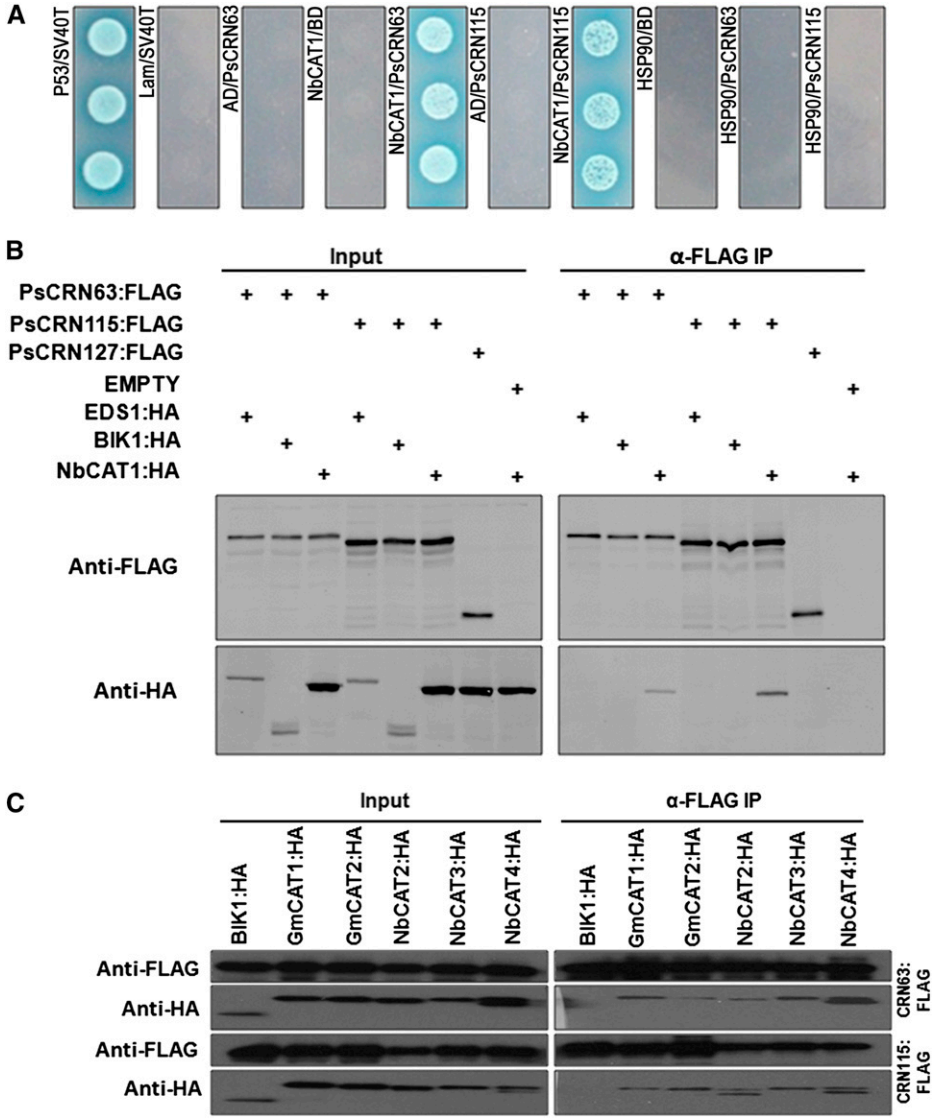

Figure 2. PsCRN63 and PsCRN115 interact with plant catalases. A, Interaction between PsCRN63 and PsCRN115 (lacking the predicated signal peptides) with NbCAT1 in yeast two-hybrid assays. Yeast transformants expressing the indicated genes were plated on synthetic dextrose/-Trp-Leu-His-adenine medium containing 5-bromo-4-chloro-3-indolyl-α-D-galactopyranoside. B, co-IP of PsCRN63 or PsCRN115 with NbCAT1. PsCRN63:FLAG or PsCRN115:FLAG was transiently coexpressed with NbCAT1 in Arabidopsis protoplasts. The co-IP experiment was performed using anti-HA antibodies, and the isolated protein was analyzed by immunoblotting using anti-FLAG antibodies to detect PsCRN63 or PsCRN115 and anti-HA antibodies to detect NbCAT1. The *P. sojae* effector CRN127 and Arabidopsis BIK1 and EDS1 were used as negative controls. C, co-IP of PsCRN63 or PsCRN115 with other catalase homologs encoded by *N. benthamiana* and soybean. PsCRN63:FLAG or PsCRN115:FLAG was transiently coexpressed with the indicated catalases in Arabidopsis protoplasts. The co-IP experiment was performed using anti-HA antibodies, and the isolated protein was analyzed by immunoblotting using anti-FLAG antibodies to detect PsCRN63 or PsCRN115 and anti-HA antibodies to detect catalases. Arabidopsis BIK1:HA was used as a negative control.

roles in plant cell death. These roles were explored further, as described below.

PsCRN63 Promotes H_2O_2 Accumulation in *N. benthamiana* and PsCRN115 Inhibits This Activity

Since H_2O_2 is a critical trigger of plant cell death (Petrov and Van Breusegem, 2012), we tested whether the transient expression of PsCRN63 and/or PsCRN115 affects H_2O_2 accumulation in *N. benthamiana* leaves. As shown in Figure 4, H_2O_2 accumulation was significantly up-regulated in leaves expressing PsCRN63 as compared with its level in leaves expressing GFP; this up-regulation was not observed in PsCRN115-expressing leaves. Thus, PsCRN63, but not PsCRN115, promoted H_2O_2 accumulation in *N. benthamiana*. Coexpression of PsCRN63 and PsCRN115 did not alter H_2O_2 accumulation levels as compared with the GFP expression controls (Fig. 4B), suggesting that PsCRN115 inhibited the capacity of PsCRN63 to promote H_2O_2 accumulation. Since PsCRN63 and PsCRN115 have contrasting roles in manipulating PCD (Liu et al., 2011; Supplemental Fig. S2), we suggest that PsCRN63 induces plant PCD by promoting H_2O_2 accumulation, whereas PsCRN115 suppresses the process by inhibiting PsCRN63-induced H_2O_2 accumulation.

PsCRN63-Induced PCD Is Alleviated by Transient Expression of *CAT* Genes

Since catalases are responsible for the degradation of H_2O_2 (Du et al., 2008), we postulated that overexpression of catalases should alleviate the PsCRN63-triggered high accumulation of H_2O_2 and PCD. To test this postulation, we infiltrated *N. benthamiana* leaves with *PsCRN63*, *PsCRN63/PsCRN115*, *PsCRN63/GFP*, *PsCRN63/NbCAT1*, and *PsCRN63/GmCAT1* (Fig. 5A). PsCRN63 was expressed successfully in all cases

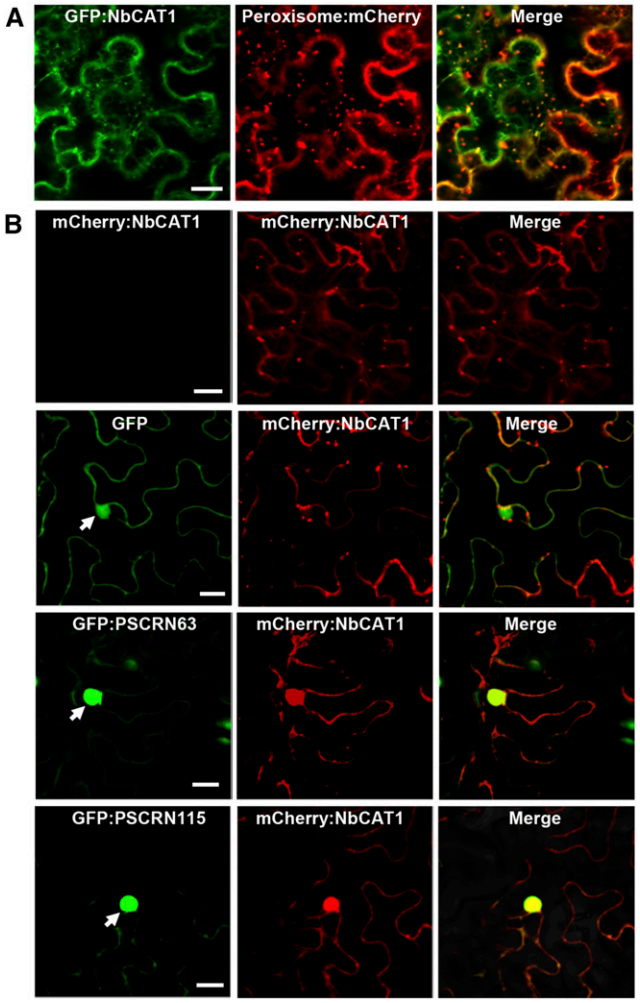

Figure 3. PsCRN63 and PsCRN115 recruit catalases into the nucleus. A, Subcellular localization of NbCAT1 in *N. benthamiana*. Agrobacterial cells containing *GFP:NbCAT1* and the peroxisome marker vector PX-RK were coinfiltrated into *N. benthamiana* leaves, and photographs were taken at 2 d after infiltration. Bar = 50 μm. B, Subcellular localization of NbCAT1. Agrobacteria harboring *mCherry:NbCAT1* were infiltrated alone or coinfiltrated with agrobacterial cells harboring *GFP*, *GFP:PsCRN63*, or *GFP:PsCRN115* into *N. benthamiana* leaves. Photographs were taken at 2 d after infiltration. Bars = 50 μm.

(Fig. 5B). PsCRN63-triggered PCD could be alleviated by transient coexpression of catalases from both *N. benthamiana* and soybean as well as by coexpression of PsCRN115 (Fig. 5A). Consistent with these results, coexpression of the plant catalases (*NbCAT1* and *GmCAT1*) or *PsCRN115* with *PsCRN63* decreased electrolyte leakage as compared with the coexpression of *PsCRN63* and *PsCRN63/GFP* (Fig. 5C). Collectively, these data showed that the PCD-inducing activity of PsCRN63 was inhibited by coexpression of its interacting protein catalases as well as of PsCRN115.

To test further whether overexpressed catalases suppress PsCRN63-induced PCD by preventing H_2O_2 accumulation, we assayed H_2O_2 levels in these infiltrated leaves using 3,3′-diaminobenzidine (DAB) staining. Very weak staining was observed in leaf areas infiltrated with *PsCRN63/NbCAT1* and *PsCRN63/GmCAT1* compared with those infiltrated with *PsCRN63* and *PsCRN63/GFP* (*PsCRN63/PsCRN115* was used as the positive control; Fig. 5D). These results indicated that overexpression of plant catalases can alleviate PsCRN63-triggered PCD by suppressing H_2O_2 levels.

To explore whether catalases also suppress PCD triggered by other inducers, we used elicitin infestin1 (INF1) from *P. infestans* (Kamoun et al., 1998), avirulence homolog241 (Avh241) from *P. sojae* (Yu et al., 2012), R/AVR pair potato (*Solanum tuberosum*) R3a (Huang et al., 2005), and *P. infestans* AVR3a (Armstrong et al., 2005). Interestingly, catalases from *N. benthamiana* and soybean did not inhibit PCD triggered by these inducers (Fig. 5E), indicating that the suppression of PsCRN63-induced PCD by catalases is specific. We also noticed that PsCRN115 did not suppress PCD triggered by these inducers (Liu et al., 2011), indicating that the catalases and PsCRN115 are specifically involved in regulating the PCD-triggering activity of PsCRN63.

Catalases Are Required for the PCD-Suppressing Activity of PsCRN115

To further test the specific interactions between catalases, PsCRN115, and PsCRN63 in regulating PCD, we silenced the *CAT* genes in *N. benthamiana* using virus-induced gene silencing (VIGS). Quantitative reverse transcription (RT)-PCR results showed that four selected *CAT* members were simultaneously down-regulated in the silenced lines compared with the control lines (Fig. 6A). The down-regulated expression of catalases did not negatively impact the PCD-triggering function

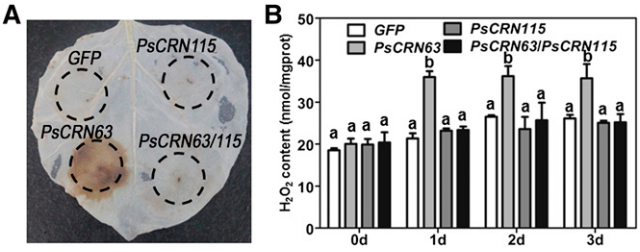

Figure 4. PsCRN63 promotes H_2O_2 accumulation, whereas PsCRN115 suppresses it, in *N. benthamiana*. A, H_2O_2 production in *N. benthamiana* leaves. DAB staining was performed at 2 d after infiltration with agrobacterial cells containing the constructs *GFP*, *PsCRN63*, *PsCRN115*, and *PsCRN63/PsCRN115*. B, H_2O_2 contents in *N. benthamiana* leaves expressing the constructs in A using the H_2O_2 detection kit. *N. benthamiana* leaves were collected at the indicated time points. Error bars represent SE from at least five biological replicates. For each time point, the same letter indicates no significant difference between values and different letters indicate significant differences between values ($P < 0.01$, nonparametric Kruskal-Wallis test).

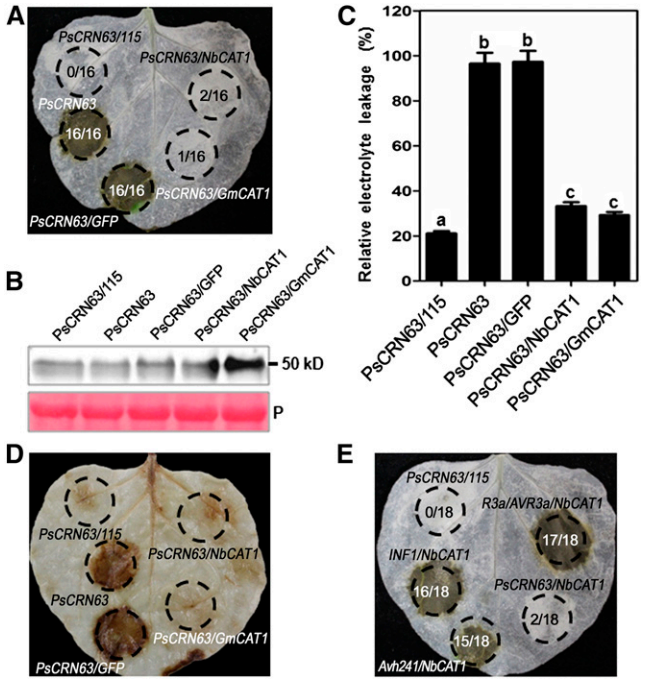

Figure 5. Transient expression of the *NbCAT1* and *GmCAT1* genes alleviates PsCRN63-triggered plant PCD. A, Suppression of PsCRN63-induced PCD by NbCAT1 and GmCAT1. GFP was used as a negative control and PsCRN115 as a positive control. Leaves of *N. benthamiana* were infiltrated with *A. tumefaciens* carrying the corresponding constructs. The photographs was taken at 4 d after infiltration. The numbers in each circled area represent summary data showing the number of infiltrated area(s) exhibiting cell death over the total number of leaf areas infiltrated with a particular construct or combination of constructs. B, The presence of the PsCRN63 protein was confirmed by immunoblotting using anti-HA antibodies. P, Ponceau S staining of the membrane to show equal loading. C, Quantification of PCD by measurement of electrolyte leakage. *N. benthamiana* leaves were agroinfiltrated with the corresponding constructs. Electrolyte leakage from the infiltrated leaf discs was measured as a percentage of leakage from boiled discs at 4 d after infiltration. Error bars represent SE calculated from five biological replicates. The same letter indicates no significant difference between values, and different letters indicate significant differences between values ($P < 0.01$, nonparametric Kruskal-Wallis test). D, H_2O_2 production in *N. benthamiana* leaves as determined by DAB staining. *N. benthamiana* leaves were infiltrated with the corresponding constructs, and the measurement was performed at 2 d after infiltration. E, Specific suppression of PsCRN63 triggered by transient expression of *NbCAT1*. *P. infestans INF1*, *P. sojae Avh241*, and *R3a/AVR3a* were used in this assay to test the specificity of PCD suppression. Photographs in D and E were taken at 4 d after infiltration. The numbers in each circled area represent summary data showing the number of infiltrated area(s) exhibiting cell death over the total number of leaf areas infiltrated with a particular construct or combination of constructs.

of PsCRN63 (Fig. 6B). This is consistent with the above results showing that an elevated expression of catalases suppressed the PCD-triggering function of PsCRN63. However, the role of PsCRN115 inhibiting PsCRN63-triggered PCD was blocked in the catalase-silenced lines (Fig. 6B), indicating that this unique role of PsCRN115 was dependent on plant catalases. In contrast, transient expression of GFP did not trigger PCD at 4 d after infiltration (Fig. 6B).

PsCRN63 Affects the Stability of Catalase Proteins

The above results showing that PsCRN63-induced PCD was alleviated by overexpression of catalases and that PsCRN63 still induced PCD in catalase-silenced plants raised the possibility that one mechanism of PsCRN63 induction of PCD is decreased levels of catalases in the presence of PsCRN63. Furthermore, PsCRN115 may counteract this effect by maintaining or elevating the catalase levels. To test these possibilities, we investigated whether these CRN effectors

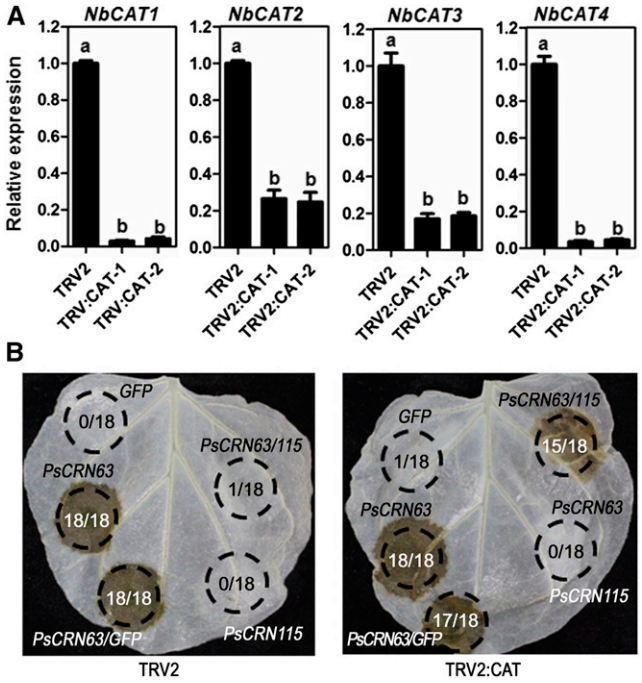

Figure 6. The suppression of PsCRN63-triggered PCD of PsCRN115 is dependent on plant catalases. A, Relative *CAT* gene expression levels in VIGS and control *N. benthamiana* determined by real-time PCR. TRV2:CAT-1 and TRV2:CAT-2 represent two independent VIGS plants, and TRV2 represents the empty vector control plants. *NbEF1α* and *NbACTIN* genes were used as reference genes. The same letter indicates no significant difference between values, and different letters indicate significant differences between values ($P < 0.01$, nonparametric Kruskal-Wallis test). B, Loss of PsCRN115 suppression of PsCRN63-triggered PCD in *CAT*-silenced *N. benthamiana*. Agrobacterial cells carrying the *PsCRN115* construct were infiltrated into *CAT*-silenced *N. benthamiana* leaves 12 h prior to infiltration with agrobacterial cells harboring the *PsCRN63* construct. Photographs were taken at 4 d after infiltration. GFP was used as a negative control. The numbers in each circled area represent summary data showing the number of infiltrated area(s) exhibiting cell death over the total number of leaf areas infiltrated with a particular construct or combination of constructs.

affected catalase stability. We coinfiltrated the *Agrobacterium tumefaciens* strain carrying the GFP:CRN construct with that containing the CAT:HA (for hemagglutinin) construct into *N. benthamiana* leaves and extracted total proteins from the treated leaves 2 d after infiltration. Western-blot analysis revealed that the protein level of NbCAT1:HA or GmCAT1:HA was significantly lower when PsCRN63 was coexpressed than in the control in which GFP was coexpressed (Fig. 7A). When catalase was coexpressed with PsCRN63 and PsCRN115, the protein stability in infiltrated leaves was recovered compared with those expressing only PsCRN63 (Fig. 7A), suggesting that PsCRN115 protects catalases from destabilization by PsCRN63. To test whether the degradation of catalases by PsCRN63 was dependent on the 26S proteasome, we analyzed their stability in the presence of MG132, which is an inhibitor of the 26S proteasome. The result showed that the degradation of catalases was not alleviated by treatment with MG132 compared with that treated with dimethyl sulfoxide (Fig. 7A). Thus, destabilization of catalases by PsCRN63 is likely independent of the 26S proteasome pathway.

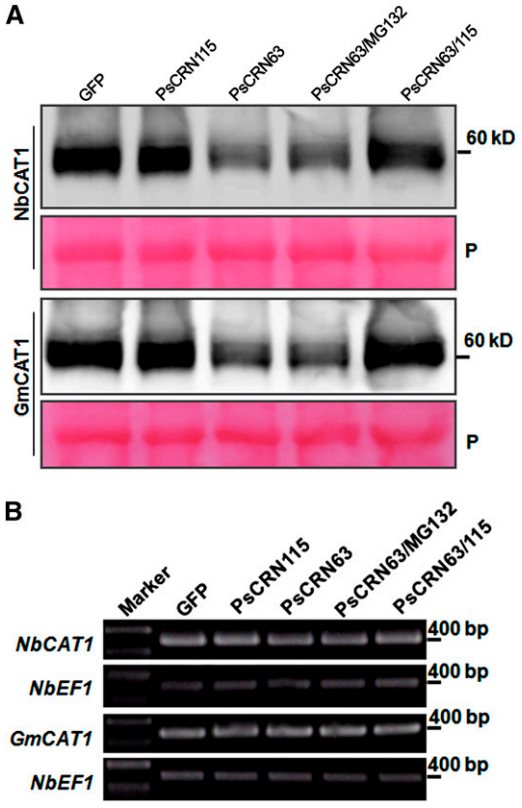

Figure 7. PsCRN63 destabilizes catalase in *N. benthamiana*. A, Analysis of the protein stability of NbCAT1 and GmCAT1 using western blotting. Total protein was extracted from each sample collected and immunoblotted using anti-HA antibodies to detect NbCAT1 or GmCAT1. Agrobacterial cells carrying the *NbCAT1:HA* or *GmCAT1:HA* construct were coinfiltrated into *N. benthamiana* leaves with cells carrying *GFP*, *PsCRN63*, or *PsCRN115* (without the secretory signal peptide). In both experiments, leaves were treated with MG132 (100 μM; as indicated) or dimethyl sulfoxide (other lanes) 1 d after infiltration with agrobacterial cells. The infiltrated leaves were harvested 1 d after treatment with MG132 or dimethyl sulfoxide. P, Ponceau S staining of the membrane to show equal loading. B, Transcriptional levels of each gene determined by RT-PCR. Total RNA was isolated from infiltrated *N. benthamiana* leaves. The expression levels of *NbCAT1* or *GmCAT1* in infiltrated leaves were detected by RT-PCR. *N. benthamiana NbEF1α* was used as a reference gene.

To exclude the possibility that the destabilization of catalase by PsCRN63 was a general consequence of PCD, we stained the total proteins used in the western-blot experiment. Clear and sharp protein bands were observed for all samples tested, indicating that the degradation of catalases was not due to quality problem of the total proteins (Fig. 7A). To test whether the difference in the catalase protein contents in the presence and absence of PsCRN63 was caused by differential transcriptional expression of *CAT* genes, we analyzed the *NbCAT1* and *GmCAT1* mRNA abundance using RT-PCR and found no significant difference in the transcription levels of these genes among samples (Fig. 7B).

Taken together, these data suggest that PsCRN63 may induce PCD by reducing the stability of catalases and that PsCRN115 may suppress PsCRN63-triggered PCD by suppressing its catalase-destabilizing activity. How can this model explain the observation that PsCRN63 could still induce PCD in the catalase-silenced plants? It is possible that catalase accumulation needs to reach a threshold low level to allow high enough H_2O_2 accumulation to trigger PCD and that PsCRN63 acted to reduce catalase in the silenced plants to reach this threshold low level. Another possibility is that PsCRN63 interacts with a yet-to-be identified host factor, in addition to reducing the catalase level (and elevating H_2O_2), to trigger PCD. Whether relocating the catalase to the nucleus to interact with this putative factor remains an outstanding question.

Plant Catalases Contribute to Resistance against *Phytophthora* spp. Pathogens

To determine whether *CAT* genes are responsive to *Phytophthora* spp. infection, we used real-time PCR to detect *CAT* gene expression in *N. benthamiana* leaves challenged with *P. capsici* zoospores. The expression levels of *NbCAT1* and *NbCAT2* were significantly upregulated in response to *P. capsici* inoculation, indicating that the catalases may be involved in plant resistance to *Phytophthora* spp. pathogens (Fig. 8A). However, the expression of *NbCAT3* and *NbCAT4* was not induced during *Phytophthora* spp. infection (Fig. 8A).

To examine the role of catalases in resistance to *Phytophthora* spp. pathogens, we silenced four *CAT* genes simultaneously in *N. benthamiana* using the VIGS approach (Fig. 5A). The inoculation assay results showed that the catalase-silenced plants were more susceptible to *P. capsici* than the TRV2 control lines

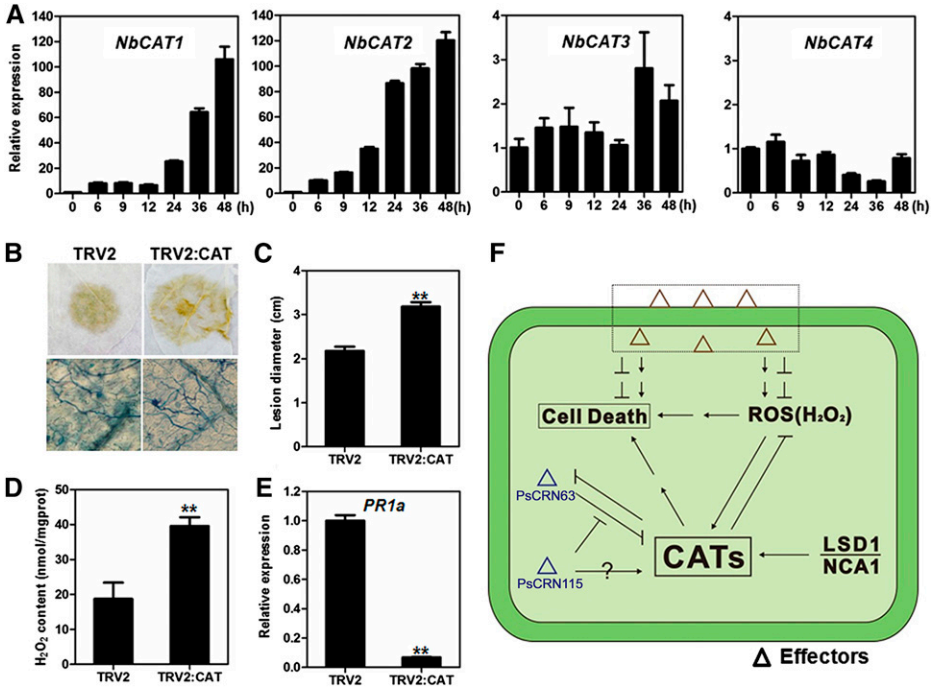

Figure 8. Silencing of *CAT* genes in *N. benthamiana* reduces resistance to *P. capsici*. A, Relative expression of *CAT* genes in *N. benthamiana* at 0, 6, 9, 12, 24, 36, and 48 h after inoculation with *P. capsici*. Relative expression levels were standardized to that of the *NbEF1α* and *NbACTIN* reference genes. B, Comparison of *P. capsici* lesions on *N. benthamiana* leaves expressing the TRV2:CAT or TRV2 construct. The top row shows decolorized infected leaves at 24 h after inoculation. The bottom row shows Trypan Blue staining of lesions, revealing a higher hyphal density in the *CAT*-silenced *N. benthamiana*. C, Average lesion diameters of *N. benthamiana* leaves expressing the TRV2:CAT or TRV2 construct. Error bars represent SE calculated from 12 biological replicates (**$P < 0.01$, Student's *t* test). D, H_2O_2 production in *CAT*-silenced and control *N. benthamiana*. Error bars represent SE calculated from four biological replicates (**$P < 0.01$, Student's *t* test). E, Relative expression levels of the *PR1a* gene in *CAT*-silenced *N. benthamiana* and control lines. Error bars represent SE calculated from three biological replicates (**$P < 0.01$, Student's *t* test). F, Model for the manipulation of plant PCD by PsCRN63 and PsCRN115 through interactions with plant CATs. Pathogens produce effectors to induce or suppress PCD and ROS in plant cells. *P. sojae* secretes PsCRN63 to interact with plant catalases, which elevates H_2O_2 levels in plant cells and causes PCD. At the same time, *P. sojae* produces relatively lower amounts of PsCRN115 to suppress the PsCRN63-induced PCD by recovering the catalase activity. To overcome this manipulation by the pathogen, plants up-regulate the expression of catalases, which in turn suppresses the PsCRN63 activity and leads to resistance against the oomycete pathogen *P. sojae*.

(Fig. 8, B and C). To investigate the effect of silencing on plant H_2O_2 accumulation, we measured the H_2O_2 content in the catalase-silenced lines; as expected, the H_2O_2 level was higher than in control plants (Fig. 8D). Expression of the *PATHOGENESIS-RELATED 1a (PR1a)* gene, a marker for salicylic acid-mediated plant defense, was significantly down-regulated in the catalase-silenced plants compared with the control lines (Fig. 8E). Therefore, we showed that catalases positively regulate plant resistance to *Phytophthora* spp. pathogens.

DISCUSSION AND CONCLUSION

PCD plays a central role in plant innate immune systems. Recognition of the pathogen by plant nucleotide-binding oligomerization domain-like receptors often leads to the hypersensitive response (a form of PCD). The hypersensitive response may prevent pathogen growth and/or generate long-range signals for systemic acquired resistance, although disease resistance and the hypersensitive response can be uncoupled in some cases (Coll et al., 2011). *Phytophthora* spp. pathogens likely evade host PCD during the biotrophic phase but promote it during the necrotrophic phase. A wide range of secreted proteins from *Phytophthora* spp. pathogens have been identified as modulators of host PCD (Kamoun, 2006). However, the mechanisms by which host PCD is manipulated by these proteins remain unknown. We previously demonstrated that PsCRN63 and PsCRN115, although sharing high sequence similarity, have contrasting roles in manipulating plant PCD. Expression of PsCRN63 and PsCRN115 is jointly required for full virulence (Liu et al., 2011). Here, we show that expression of *PsCRN63* or *PsCRN63/115* together promotes the in planta growth of *P. capsici*. PsCRN63 and PsCRN115 both interact with *N. benthamiana* and soybean catalases, the essential enzymes for the plant antioxidative system. The expression of *NbCAT1* or *GmCAT1* specifically blocks PsCRN63-induced PCD in *N. benthamiana*, and

PsCRN63-induced PCD is associated with ROS accumulation. Silencing of *NbCAT* genes in *N. benthamiana* compromises the suppression of PsCRN63-induced PCD by PsCRN115. *NbCAT1* and *NbCAT2* genes are highly expressed during *N. benthamiana-P. capsici* interactions, and silencing of *NbCAT* genes accelerates pathogen infection in *N. benthamiana*. These results indicate that PsCRN63/PsCRN115 may regulate plant PCD and immune responses by interacting with plant catalases.

Plant catalase, a type of peroxisomal enzyme decomposing H_2O_2, plays essential roles in maintaining H_2O_2 homeostasis and regulating PCD in plant cells (Mhamdi et al., 2010; Fig. 8F). It was reported that the *Arabidopsis cat2* mutant exhibits increasingly intense DAB staining after infiltration with avirulent bacteria (Simon et al., 2010) and shows spreading necrotic lesions in a daylength-related manner (Chaouch et al., 2010). Little genetic evidence shows that CATs are involved in disease resistance. We observed that *CAT*-deficient *N. benthamiana* leaves, although accumulating higher levels of H_2O_2, were more susceptible to *P. capsici*. We inferred that CATs could be essential components for disease resistance by maintaining proper H_2O_2 levels in *N. benthamiana*.

CATs have opposite roles in manipulating plant PCD (Fig. 8F). On the one hand, CATs prevent PCD by detoxifying H_2O_2, which is supported by a large body of evidence (Chaouch et al., 2010; Mhamdi et al., 2010). LSD1, a negative regulator of PCD, interacts with CATs to regulate light-dependent runaway PCD and hypersensitive-type PCD (Li et al., 2013). On the other hand, CATs may promote autophagy-dependent PCD in Arabidopsis (Juul et al., 2010; Hackenberg et al., 2013). Plant catalases enter into an active state by one molecule of H_2O_2. Arabidopsis *cat2* mutants compromise hydroxyurea (an antineoplastic drug)-induced PCD, in which hydroxyurea interacts directly with catalase and inhibits its H_2O_2 decomposition activities (Juul et al., 2010). This may be because catalase activation by H_2O_2 generates a signal to activate autophagy-dependent PCD. Arabidopsis *no catalase activity1* (*nca1*) mutants exhibit extremely low catalase activities, and both *nca1* and *cat2* mutants attenuate avirulence protein Rpm1-triggerred PCD, suggesting that CAT acts as a molecular link between ROS and the promotion of autophagy-dependent PCD (Hackenberg et al., 2013). Thus, plant CATs may act as fine-tuning regulators of H_2O_2 homeostasis and H_2O_2-mediated PCD. In this regard, we speculate that *P. sojae* produces these two cytoplasmic effectors to perturb H_2O_2 homeostasis and H_2O_2-mediated PCD by interacting with the CATs (Fig. 8F). Consistently, silencing *PsCRN63/115* in *P. sojae* leads to a stronger PCD in host cells at the early infection stage than the wild-type control (Liu et al., 2011).

Interestingly, it has also been shown that the cucumber mosaic virus (CMV) 2b protein interferes directly with plant catalase activity to induce PCD, which appears to promote CMV infection (Inaba et al., 2011). Similar to the 2b protein, we show that PsCRN63 induces PCD by promoting H_2O_2 accumulation. However, the PsCRN63-CAT interaction may decrease the stability of the catalase proteins, which was not observed for the 2b-CAT interaction, suggesting that *P. sojae* PsCRN63 interference with catalases differs from that of the CMV 2b protein. The regulation of plant PCD by modulating H_2O_2 homeostasis has been adopted by other plant pathogens (Hemetsberger et al., 2012). That case offers an example of convergent evolution, in which these evolutionarily distant organisms have evolved the ability to interfere with the same targets.

The interaction between PsCRN63/115 and plant catalases appears to favor the pathogen. These two effectors together are required for the full pathogenesis of *P. sojae* by suppressing host defense responses, and these two highly similar proteins exhibit contrasting roles in the manipulation of host PCD (Liu et al., 2011). *P. sojae* is a hemibiotroph and typically switches from biotrophic to necrotrophic lifestyle at 16 to 24 h following the invasion of host tissues (Tyler, 2007). *PsCRN63* is highly expressed in each of the tested stages and induced during the late infection stages, whereas *PsCRN115* is weakly expressed and slightly down-regulated at all infection stages (Liu et al., 2011), indicating that PsCRN63 may play a dominant role during the interactions. PsCRN63 reduces the stability of catalase proteins. Consequently, the PsCRN63-CAT interaction partially compromises H_2O_2 scavenging by catalases, which enhances H_2O_2 accumulation and triggers PCD (Fig. 8F). Considering its expression patterns during infection, we suggest that PsCRN63-induced PCD by association with CATs may contribute to a hemibiotrophic lifestyle. By contrast, PsCRN115 also exhibits the ability to suppress PCD induced by *P. sojae* necrosis-inducing protein (Liu et al., 2011), which transcribes during the transition from biotrophy to necrotrophy and is highly expressed during late stages of a compatible interaction (Qutob et al., 2006). Silencing of *CAT* genes in *N. benthamiana* compromises the PCD-suppressing activity of PsCRN115, suggesting that catalases are required for the biological function of PsCRN115 (Fig. 8F). A possible explanation is that PsCRN115 suppresses PsCRN63-induced PCD by protecting plant catalases through competitive binding of catalases.

Overexpression of catalase alleviates PsCRN63-induced PCD, indicating that plants may evade the effects imposed by PsCRN63 through increasing expression of *CAT* genes (Fig. 8F). However, it does not affect PCD triggered by other inducers, such as Avh241, INF1, and R3a/AVR3a, indicating that catalases specifically suppress PsCRN63-triggered PCD. An explanation is that PsCRN63-induced PCD is dependent on the H_2O_2 signaling pathway, while the other inducers are independent of this pathway. Furthermore, silencing catalases in *N. benthamiana* leads to increased disease lesions when challenged with *P. capsici*, reinforcing the importance of catalases in

plant immunity and of manipulating catalases in *Phytophthora* spp. pathogenesis.

In conclusion, PsCRN63 and PsCRN115, although with high sequence similarity, play opposite roles in regulating plant cell death. Both effector proteins interact directly with plant catalases, which remove H_2O_2, suggesting that PsCRN63 and PsCRN115 modulate host cell death by perturbing H_2O_2 homeostasis. Indeed, PsCRN63 may alter the subcellular localization of catalases and reduce the stability of catalase proteins, therefore enhancing H_2O_2 accumulation in plant cells. PsCRN115 suppresses these processes, although it also recruits catalases in the plant nucleus. Furthermore, silencing catalases in *N. benthamiana* led to increased disease lesions when challenged with *P. capsici*, reinforcing the importance of manipulating catalases in *Phytophthora* spp. pathogenesis. Although it cannot be completely excluded that PsCRN63 and PsCRN115 may have other targets that are also involved in plant PCD, our results provide evidence that *Phytophthora* spp. pathogens may produce two CRN effectors to interfere directly with plant ROS homeostasis to manipulate PCD by hijacking plant catalases.

MATERIALS AND METHODS

Transient Expression

Agrobacterium tumefaciens strain GV3101 harboring different constructs was grown in liquid Luria-Bertani medium at 28°C in a shaking incubator at 200 rpm. After 24 h, bacterial cells were collected by centrifugation at 3,500*g* for 5 min, washed with 10 mM $MgCl_2$ three times, and resuspended in infiltration medium (10 mM $MgCl_2$, 10 mM MES, pH 5.6, and 150 μM acetosyringone) to an optical density at 600 nm of 0.4 prior to infiltration into the entire leaf or leaf sections. In experiments where different coinoculation ratios were tested, the total amount of each construct combination was an optical density at 600 nm of 0.4.

Phytophthora capsici Culture Conditions and Inoculation Procedures

The *P. capsici* isolates used in the study were routinely cultured at 25°C in the dark on 10% (v/v) V8 juice agar plates. Zoospores were obtained by incubating mycelial plugs in 10% (v/v) V8 broth at 25°C for 2 d and then washed three times with sterilized water. After 12 h, numerous sporangia developed. To release zoospores, the cultures were treated in cold sterilized water for 0.5 h followed by incubation at 25°C for 1 h (Zhang et al., 2012). Infection assays were performed using droplet inoculations of zoospore solutions of the *P. capsici* isolate (10 μL of a 50,000 zoospores mL^{-1} solution) on detached *Nicotiana benthamiana* leaves. To compare *CAT*-silenced *N. benthamiana* and the empty vector control, detached leaves at 10 d after infiltration were challenged with *P. capsici* zoospores. To evaluate the virulence function of PsCRN63 or PsCRN115, *N. benthamiana* leaves were agroinfiltrated with the binary vector pBinGFP2 (expressing free GFP) on one-half of the leaf and the recombinant pBinGFP2 vector containing CRN effector was agroinfiltrated on the other half of the same leaf. The infiltrated leaves were inoculated with *P. capsici* zoospores 12 h after infiltration. The lesion size was measured 24 h after inoculation. The assay was repeated at least three times.

co-IP Experiments and LC-MS/MS Analysis

For co-IP experiments, total protein was extracted from *N. benthamiana* leaves 2 to 5 d after infiltration of the PVX:PsCRN63:HA or PVX:PsCRN115:HA construct and subjected to immunoprecipitation using the HA Tag IP/Co-IP Kit (Pierce), as per the manufacturer's protocol.

The preparation of peptides for LC-MS/MS was performed as follows. Briefly, each protein sample was cleaned and digested in gel using sequencing-grade modified trypsin. The resulting peptide mixtures were analyzed by an LC-MS/MS system, in which HPLC using a 75-μm i.d. reverse-phase C18 column was coupled with an ion-trap mass spectrometer. The mass spectrometric data acquired were used to search a nonredundant protein database. The output from the database search was validated manually before reporting.

Arabidopsis Protoplast Isolation, Transfection, and co-IP

The Columbia ecotype of Arabidopsis (*Arabidopsis thaliana*) was used for protoplast isolation. The plants were grown for 4 to 5 weeks in a 10-h-light/14-h-dark photoperiod at 22°C. Leaves (approximately 0.5 g) from plants were collected and cut into 0.5- to 1-mm strips with a fresh razor blade. Leaf sections were transferred to a petri dish containing 10 mL of enzyme solution (1% [w/v] cellulose R10, 0.2% [w/v] macerozyme R10, 0.4 M mannitol, 20 mM KCl, 10 mM $CaCl_2$, and 0.1% [w/v] bovine serum albumin) and gently shaken (40 rpm on a platform shaker) for 3 h. The protoplasts were filtered (200-μm nylon mesh) and pelleted at 100*g* for 3 min. The protoplasts were then washed twice with W5 solution (154 mM NaCl, 125 mM $CaCl_2$, 5 mM KCl, and 2 mM MES, pH 5.7), repelleted and resuspended gently in W5 solution, and incubated on ice for 30 min. The protoplasts were collected and resuspended in MMg solution (0.4 M mannitol, 15 mM $MgCl_2$, and 4 mM MES, pH 5.7) at 3×10^5 protoplasts mL^{-1} for experiments requiring transfected genes. Protoplasts were transfected by a polyethylene glycol method. Briefly, 6×10^4 protoplasts in 0.2 mL of MMg solution were mixed at room temperature with 10 μg of supercoiled plasmid. An equal volume of polyethylene glycol 4000 solution (40% [w/v] polyethylene glycol 4000, 0.2 M mannitol, and 0.1 M $CaCl_2$) was added, and the mixture was incubated at room temperature for 7 min. After incubation, 1 mL of W5 solution was added slowly and pelleted by centrifugation at 100*g* for 3 min. The protoplasts were washed twice with W5 solution and incubated for 16 h under weak light. For the co-IP assay, the total proteins were extracted from Arabidopsis protoplasts expressing the indicated genes in extraction buffer (50 mM HEPES-KOH, pH 7.5, 150 mM KCl, 1 mM EDTA, 0.5% [v/v] Triton X-100, 1 mM dithiothreitol, and 1× protease inhibitor cocktail). After centrifugation at 13,000 rpm for 15 min, anti-FLAG antibody-couple beads (Sigma-Aldrich) were subsequently added and incubated for 4 h at 4°C. After washing the beads six times with extraction buffer, immunoprecipitates were analyzed by western-blot analysis.

Yeast Two-Hybrid Assay

The yeast (*Saccharomyces cerevisiae*) two-hybrid assay was performed according to the Matchmaker Two-Hybrid System 3 protocol (Clontech). *PsCRN63* and *PsCRN115* lacking the signal peptides were amplified with the primer pairs CRN63F_*Eco*RI/CRN63R_*Bam*HI and CRN115F_*Eco*RI/CRN63R_*Bam*HI, respectively (Supplemental Table S2). The PCR products were inserted into pGBKT7 as the bait vectors. *NbCAT1* was amplified using the primer pair NbC1-Y-F/NbC1-Y-R (Supplemental Table S2) and inserted into pGADT7 as the prey vector. The resulting pGADT7-NbCAT1 and each bait vector were cotransformed into the yeast strain AH109. Transformants that appeared on synthetic dextrose/-Trp-Leu medium were isolated and assayed for growth on synthetic dextrose/-Trp-Leu-His-adenine plates supplemented with 5-bromo-4-chloro-3-indolyl-α-D-galactopyranoside.

Sequence Analysis

The homologous catalases in *N. benthamiana* and soybean (*Glycine max*) were identified by BLAST using the *N. benthamiana* genome database (http://solgenomics.net/organism/Nicotiana_benthamiana/genome) or the soybean genome database (http://www.plantgdb.org/GmGDB/cgi-bin/blastGDB.pl). Sequence alignment was performed using MUSCLE software (Edgar, 2004).

Confocal Laser Scanning Microscopy

N. benthamiana leaf tissue was mounted in water under a coverslip at 48 h after infiltration with *A. tumefaciens* carrying the corresponding constructs. Images were captured using the Zeiss LSM 710 confocal laser scanning microscope. The GFP constructs were excited at 488 nm, and the mCherry constructs were excited at 561 nm. Images were processed using the Zeiss LSM 710 confocal laser scanning microscope and Adobe Photoshop software packages.

DAB Staining and H_2O_2 Measurement

H_2O_2 was detected in situ using DAB staining (Thordal-Christensen et al., 1997) with some modifications. *N. benthamiana* leaves were infiltrated with the

recombinant *A. tumefaciens* suspension. Detached leaf samples were collected 3 d after infiltration with 1 mg mL^{-1} DAB solution. The sampled leaves were placed in a plastic box within a constant-temperature incubator for 4 h; they were then fixed in 95% (v/v) ethanol and photographed.

Quantitative measurement of H_2O_2 production was performed using the H_2O_2 detection kit (Jiancheng Bioengineering Institute). The principle of the kit is to generate a stable chelating material through the interaction between H_2O_2 and molybdic acid. The optical density of this material was measured at 405 nm. The infiltrated *N. benthamiana* leaves were harvested, and H_2O_2 accumulation was assayed following the manufacturer's instructions.

Protein Extraction and Western Blotting

Proteins were transiently expressed by *A. tumefaciens* in *N. benthamiana* leaves and harvested 2 d after infiltration. Immunoblot analyses were performed on protein extracts prepared by grinding 400 mg of leaf tissues in 1 mL of extraction buffer (50 mM HEPES-KOH, pH 7.5, 150 mM KCl, 1 mM EDTA, 0.5% [v/v] Triton X-100, 1 mM dithiothreitol, and 1× protease inhibitor cocktail). Suspensions were mixed and centrifuged at 12,000*g* for 15 min at 4°C. Protein concentration was measured using the Bradford assay. Proteins from the sample lysates were fractionated using SDS-PAGE. After electrophoresis, proteins were transferred from the gel to an Immobilon P^{SQ} polyvinylidene difluoride membrane. The membrane was washed in PBST (phosphate-buffered saline with 0.1% [v/v] Tween 20) for 2 min, and the membrane was then blocked in PBSTM (phosphate-buffered saline with 0.1% [v/v] Tween 20 and 5% [w/v] nonfat dry milk) for 1 h. Mouse anti-HA monoclonal antibodies (Sigma-Aldrich) were added to the PBSTM at a ratio of 1:5,000 and incubated at room temperature for 90 min, followed by three washes (5 min each) with PBST. The membrane was then incubated with goat anti-mouse IRDye 800CW (Odyssey [no. 926-32210]; Li-Cor) at a ratio of 1: 8,000 in PBSTM at room temperature for 30 min with shaking. The membrane was washed three times (5 min each) with PBST and then visualized using Odyssey with excitation at 700 and 800 nm.

Measurement of Ion Leakage

Ion leakage is an indicator of PCD. In this study, PCD was assayed based on measuring ion leakage from leaf discs. For each measurement, five leaf discs (9 mm in diameter) were floated on 5 mL of distilled water for 3 h at room temperature. The conductivity of the bathing solution was then measured using a conductivity meter (Con 700; Consort) to obtain value A. The leaf discs were then transferred to the bathing solution and boiled in sealed tubes for 25 min, after which the conductivity was measured again to obtain value B. For each measurement, ion leakage was expressed as a percentage: (value A/value B) × 100.

VIGS of Catalases in *N. benthamiana*

We used the TRV-based VIGS system, which uses bipartite sense RNA1 and RNA2 viruses (Liu et al., 2002), to silence *CAT* genes in *N. benthamiana*. The *NbCAT1* fragment was amplified by PCR and then cloned into pTRV2. Primer pairs NbCF_*Sma*I and NbCR_*Xba*I (Supplemental Table S2) were used to amplify *NbCAT1*. The construct was sequenced to confirm cloning accuracy. Wild-type *N. benthamiana* plants were grown in a growth chamber under a 16-h-light/8-h-dark photoperiod at 23°C. At the three- to four-leaf stage, the *N. benthamiana* plants were selected for agroinfiltration. Prior to agroinfiltration, *A. tumefaciens* GV3101 cells carrying pTRV1 and pTRV2 constructs were collected and resuspended in infiltration medium (10 mM $MgCl_2$, 10 mM MES, pH 5.6, and 150 μM acetosyringone) and mixed in a 1:1 ratio. Plants were kept in high humidity for 24 h and then grown for approximately 2 weeks after infiltration with TRV. The fully expanded six to eight leaves of the silenced plants were then used for real-time PCR and inoculation assays. VIGS of the *N. benthamiana* phytoene desaturase was used as an indicator of effective silencing (Liu et al., 2002). The empty TRV2 vector was used as the negative control.

RNA Extraction and Transcript Level Analysis

Total RNA was isolated using Trizol reagent (Invitrogen) from *N. benthamiana* leaves. Total RNA was treated with DNase I (TaKaRa) before being used for complementary DNA (cDNA) synthesis. To generate first-strand cDNA, 1 μg of total RNA was reverse transcribed in a 20-μL volume using the PrimeScript RT reagent kit according to the manufacturer's instructions (TaKaRa).

For gene transcript level analysis, SYBR Green quantitative RT-PCR assays were conducted. Primer pairs (Supplemental Table S2) were designed for each of the selected genes. The *N. benthamiana elongation factor 1α* (*NbEF1α*) and *NbACTIN* genes were used as internal controls. Quantitative RT-PCR was performed in a 20-μL reaction including 20 ng of cDNA, 0.2 μM gene-specific primer, 0.4 μL of ROX Reference Dye, 10 μL of SYBR Premix ExTaq (TaKaRa), and 6.8 μL of deionized water. Reactions were performed on an ABI PRISM 7500 Fast Real-Time PCR System (Applied Biosystems) under the following conditions: 95°C for 30 s, then 40 cycles at 95°C for 5 s and 60°C for 34 s, followed by 95°C for 15 s and 60°C for 1 min, and then 95°C for 15 s to obtain melt curves. The relative transcript abundance of each gene was determined using the delta-delta Ct method employing the formula: relative expression = $2^{-[\Delta Ct\ test - \Delta Ct\ calibrator]}$ where Ct refers to the threshold cycle, test indicates the treated sample, and calibrator indicates the control sample. Gene expression was normalized against the geometric average of two housekeeping genes (*NbEF1α* and *NbACTIN*; Vandesompele et al., 2002).

Trypan Blue Staining

For the detection of cell death, Trypan Blue staining was performed. A Trypan Blue stock solution was prepared by mixing 10 g of phenol, 10 mL of glycerol, 10 mL of lactic acid, 10 mL of distilled water, and 0.02 g of Trypan Blue. *N. benthamiana* leaves soaking in Trypan Blue solution were boiled in a water bath for 2 min and incubated for 1 d. After destaining in saturated chloral hydrate solution (2.5 g of chloral hydrate per 1 mL of water) for 2 d, samples were equilibrated with 70% (v/v) glycerol for photography.

Supplemental Data

The following supplemental materials are available.

Supplemental Figure S1. Protein sequence alignment of the catalases from *N. benthamiana* and *G. max*.

Supplemental Figure S2. Cell-death manipulation assay of CRN:GFP fusion proteins.

Supplemental Table S1. Plant proteins that may associate with PsCRN63 or PsCRN115 after co-IP as identified by mass spectrometry.

Supplemental Table S2. Oligonucleotides used for PCR and plasmid construction.

ACKNOWLEDGMENTS

We thank Biao Ding (Ohio State University) for editing the article, and Brett Tyler (Oregon State University) and Xiaofeng Cui (Shanghai Institutes for Biological Sciences) for constructive suggestions.

Received October 26, 2014; accepted November 23, 2014; published November 25, 2014.

LITERATURE CITED

Armstrong MR, Whisson SC, Pritchard L, Bos JI, Venter E, Avrova AO, Rehmany AP, Böhme U, Brooks K, Cherevach I, et al (2005) An ancestral oomycete locus contains late blight avirulence gene Avr3a, encoding a protein that is recognized in the host cytoplasm. Proc Natl Acad Sci USA **102:** 7766–7771

Bos JIB, Armstrong MR, Gilroy EM, Boevink PC, Hein I, Taylor RM, Zhendong T, Engelhardt S, Vetukuri RR, Harrower B, et al (2010) *Phytophthora infestans* effector AVR3a is essential for virulence and manipulates plant immunity by stabilizing host E3 ligase CMPG1. Proc Natl Acad Sci USA **107:** 9909–9914

Bouwmeester K, de Sain M, Weide R, Gouget A, Klamer S, Canut H, Govers F (2011) The lectin receptor kinase LecRK-I.9 is a novel *Phytophthora* resistance component and a potential host target for a RXLR effector. PLoS Pathog **7:** e1001327

Bozkurt TO, Schornack S, Win J, Shindo T, Ilyas M, Oliva R, Cano LM, Jones AME, Huitema E, van der Hoorn RAL, et al (2011) *Phytophthora infestans* effector AVRblb2 prevents secretion of a plant immune protease at the haustorial interface. Proc Natl Acad Sci USA **108:** 20832–20837

Chaouch S, Queval G, Vanderauwera S, Mhamdi A, Vandorpe M, Langlois-Meurinne M, Van Breusegem F, Saindrenan P, Noctor G

(2010) Peroxisomal hydrogen peroxide is coupled to biotic defense responses by ISOCHORISMATE SYNTHASE1 in a daylength-related manner. Plant Physiol **153:** 1692–1705

Coll NS, Epple P, Dangl JL (2011) Programmed cell death in the plant immune system. Cell Death Differ **18:** 1247–1256

Dong S, Yin W, Kong G, Yang X, Qutob D, Chen Q, Kale SD, Sui Y, Zhang Z, Dou D, et al (2011) *Phytophthora sojae* avirulence effector Avr3b is a secreted NADH and ADP-ribose pyrophosphorylase that modulates plant immunity. PLoS Pathog **7:** e1002353

Dou D, Zhou JM (2012) Phytopathogen effectors subverting host immunity: different foes, similar battleground. Cell Host Microbe **12:** 484–495

Du YY, Wang PC, Chen J, Song CP (2008) Comprehensive functional analysis of the *catalase* gene family in *Arabidopsis thaliana*. J Integr Plant Biol **50:** 1318–1326

Edgar RC (2004) MUSCLE: multiple sequence alignment with high accuracy and high throughput. Nucleic Acids Res **32:** 1792–1797

Gough DR, Cotter TG (2011) Hydrogen peroxide: a Jekyll and Hyde signalling molecule. Cell Death Dis **2:** e213

Haas BJ, Kamoun S, Zody MC, Jiang RHY, Handsaker RE, Cano LM, Grabherr M, Kodira CD, Raffaele S, Torto-Alalibo T, et al (2009) Genome sequence and analysis of the Irish potato famine pathogen *Phytophthora infestans*. Nature **461:** 393–398

Hackenberg T, Juul T, Auzina A, Gwizdz S, Malolepszy A, Van Der Kelen K, Dam S, Bressendorff S, Lorentzen A, Roepstorff P, et al (2013) Catalase and *NO CATALASE ACTIVITY1* promote autophagy-dependent cell death in *Arabidopsis*. Plant Cell **25:** 4616–4626

Hann DR, Gimenez-Ibanez S, Rathjen JP (2010) Bacterial virulence effectors and their activities. Curr Opin Plant Biol **13:** 388–393

Hemetsberger C, Herrberger C, Zechmann B, Hillmer M, Doehlemann G (2012) The *Ustilago maydis* effector Pep1 suppresses plant immunity by inhibition of host peroxidase activity. PLoS Pathog **8:** e1002684

Huang S, van der Vossen EA, Kuang H, Vleeshouwers VG, Zhang N, Borm TJ, van Eck HJ, Baker B, Jacobsen E, Visser RG (2005) Comparative genomics enabled the isolation of the R3a late blight resistance gene in potato. Plant J **42:** 251–261

Inaba J, Kim BM, Shimura H, Masuta C (2011) Virus-induced necrosis is a consequence of direct protein-protein interaction between a viral RNA-silencing suppressor and a host catalase. Plant Physiol **156:** 2026–2036

Juul T, Malolepszy A, Dybkaer K, Kidmose R, Rasmussen JT, Andersen GR, Johnsen HE, Jørgensen JE, Andersen SU (2010) The *in vivo* toxicity of hydroxyurea depends on its direct target catalase. J Biol Chem **285:** 21411–21415

Kamoun S (2006) A catalogue of the effector secretome of plant pathogenic oomycetes. Annu Rev Phytopathol **44:** 41–60

Kamoun S, van West P, Vleeshouwers VG, de Groot KE, Govers F (1998) Resistance of *Nicotiana benthamiana* to *Phytophthora infestans* is mediated by the recognition of the elicitor protein INF1. Plant Cell **10:** 1413–1426

Kelley BS, Lee SJ, Damasceno CMB, Chakravarthy S, Kim BD, Martin GB, Rose JKC (2010) A secreted effector protein (SNE1) from *Phytophthora infestans* is a broadly acting suppressor of programmed cell death. Plant J **62:** 357–366

Koeck M, Hardham AR, Dodds PN (2011) The role of effectors of biotrophic and hemibiotrophic fungi in infection. Cell Microbiol **13:** 1849–1857

Li Y, Chen L, Mu J, Zuo J (2013) LESION SIMULATING DISEASE1 interacts with catalases to regulate hypersensitive cell death in Arabidopsis. Plant Physiol **163:** 1059–1070

Liu T, Ye W, Ru Y, Yang X, Gu B, Tao K, Lu S, Dong S, Zheng X, Shan W, et al (2011) Two host cytoplasmic effectors are required for pathogenesis of *Phytophthora sojae* by suppression of host defenses. Plant Physiol **155:** 490–501

Liu Y, Schiff M, Marathe R, Dinesh-Kumar SP (2002) Tobacco Rar1, EDS1 and NPR1/NIM1 like genes are required for N-mediated resistance to tobacco mosaic virus. Plant J **30:** 415–429

McLellan H, Boevink PC, Armstrong MR, Pritchard L, Gomez S, Morales J, Whisson SC, Beynon JL, Birch PRJ (2013) An RxLR effector from *Phytophthora infestans* prevents re-localisation of two plant NAC transcription factors from the endoplasmic reticulum to the nucleus. PLoS Pathog **9:** e1003670

Mhamdi A, Queval G, Chaouch S, Vanderauwera S, Van Breusegem F, Noctor G (2010) Catalase function in plants: a focus on *Arabidopsis* mutants as stress-mimic models. J Exp Bot **61:** 4197–4220

Nelson BK, Cai X, Nebenführ A (2007) A multicolored set of *in vivo* organelle markers for co-localization studies in *Arabidopsis* and other plants. Plant J **51:** 1126–1136

Petrov VD, Van Breusegem F (2012) Hydrogen peroxide: a central hub for information flow in plant cells. AoB Plants **2012:** pls014

Qutob D, Kemmerling B, Brunner F, Küfner I, Engelhardt S, Gust AA, Luberacki B, Seitz HU, Stahl D, Rauhut T, et al (2006) Phytotoxicity and innate immune responses induced by Nep1-like proteins. Plant Cell **18:** 3721–3744

Rafiqi M, Ellis JG, Ludowici VA, Hardham AR, Dodds PN (2012) Challenges and progress towards understanding the role of effectors in plant-fungal interactions. Curr Opin Plant Biol **15:** 477–482

Rajput NA, Zhang M, Ru Y, Liu T, Xu J, Liu L, Mafurah JJ, Dou D (2014) *Phytophthora sojae* effector PsCRN70 suppresses plant defenses in *Nicotiana benthamiana*. PLoS ONE **9:** e98114

Saunders DGO, Breen S, Win J, Schornack S, Hein I, Bozkurt TO, Champouret N, Vleeshouwers VGAA, Birch PRJ, Gilroy EM, et al (2012) Host protein BSL1 associates with *Phytophthora infestans* RXLR effector AVR2 and the *Solanum demissum* immune receptor R2 to mediate disease resistance. Plant Cell **24:** 3420–3434

Schornack S, van Damme M, Bozkurt TO, Cano LM, Smoker M, Thines M, Gaulin E, Kamoun S, Huitema E (2010) Ancient class of translocated oomycete effectors targets the host nucleus. Proc Natl Acad Sci USA **107:** 17421–17426

Shen D, Liu T, Ye W, Liu L, Liu P, Wu Y, Wang Y, Dou D (2013) Gene duplication and fragment recombination drive functional diversification of a superfamily of cytoplasmic effectors in *Phytophthora sojae*. PLoS ONE **8:** e70036

Simon C, Langlois-Meurinne M, Bellvert F, Garmier M, Didierlaurent L, Massoud K, Chaouch S, Marie A, Bodo B, Kauffmann S, et al (2010) The differential spatial distribution of secondary metabolites in *Arabidopsis* leaves reacting hypersensitively to *Pseudomonas syringae* pv. *tomato* is dependent on the oxidative burst. J Exp Bot **61:** 3355–3370

Stam R, Jupe J, Howden AJM, Morris JA, Boevink PC, Hedley PE, Huitema E (2013) Identification and characterisation CRN effectors in *Phytophthora capsici* shows modularity and functional diversity. PLoS ONE **8:** e59517

Thordal-Christensen H, Zhang ZG, Wei YD, Collinge DB (1997) Subcellular localization of H_2O_2 in plants: H_2O_2 accumulation in papillae and hypersensitive response during the barley-powdery mildew interaction. Plant J **11:** 1187–1194

Torto TA, Li S, Styer A, Huitema E, Testa A, Gow NAR, van West P, Kamoun S (2003) EST mining and functional expression assays identify extracellular effector proteins from the plant pathogen *Phytophthora*. Genome Res **13:** 1675–1685

Tyler BM (2007) *Phytophthora sojae*: root rot pathogen of soybean and model oomycete. Mol Plant Pathol **8:** 1–8

van Damme M, Bozkurt TO, Cakir C, Schornack S, Sklenar J, Jones AM, Kamoun S (2012) The Irish potato famine pathogen *Phytophthora infestans* translocates the CRN8 kinase into host plant cells. PLoS Pathog **8:** e1002875

Vandesompele J, De Preter K, Pattyn F, Poppe B, Van Roy N, De Paepe A, Speleman F (2002) Accurate normalization of real-time quantitative RT-PCR data by geometric averaging of multiple internal control genes. Genome Biol **3:** RESEARCH0034.1–RESEARCH0034.11

Wang Q, Han C, Ferreira AO, Yu X, Ye W, Tripathy S, Kale SD, Gu B, Sheng Y, Sui Y, et al (2011) Transcriptional programming and functional interactions within the *Phytophthora sojae* RXLR effector repertoire. Plant Cell **23:** 2064–2086

Yu X, Tang J, Wang Q, Ye W, Tao K, Duan S, Lu C, Yang X, Dong S, Zheng X, et al (2012) The RxLR effector Avh241 from *Phytophthora sojae* requires plasma membrane localization to induce plant cell death. New Phytol **196:** 247–260

Zhang M, Meng Y, Wang Q, Liu D, Quan J, Hardham AR, Shan W (2012) PnPMA1, an atypical plasma membrane H^+-ATPase, is required for zoospore development in *Phytophthora parasitica*. Fungal Biol **116:** 1013–1023